JOURNAL OF GENERAL VIROLOGY

RESEARCH ARTICLE

Billington *et al.*, *Journal of General Virology* 2025;106:002150

DOI 10.1099/jgv.0.002150

MICROBIOLOGY SOCIETY

OPEN ACCESS

Investigating factors driving shifts in subtype dominance within H5Nx clade 2.3.4.4b high pathogenicity avian influenza viruses

Elizabeth Billington[1], Cecilia Di Genova[1], Caroline J. Warren[1], Saumya S. Thomas[1], Simon Johnson[1], Sofia Riccio[1], Dilhani De Silva[1], Jacob Peers-Dent[1], Nigel Temperton[2], Kelly da Costa[2], Alexander M. P. Byrne[1,†], Maisie Airey[1], Audra-Lynne Schlachter[3], Jiayun Yang[4], Alejandro Nunez[3], Munir Iqbal[4], Marek J. Slomka[1], Ian H. Brown[1,4,5], Ashley C. Banyard[1,5,*] and Joe James[1,5,*]

Abstract

H5Nx clade 2.3.4.4b high pathogenicity avian influenza viruses (HPAIVs) have decimated wild bird and poultry populations globally since the autumn of 2020. In the UK and in continental Europe, the H5N8 subtype predominated during the first epizootic wave of 2020/21, with few detections of H5N1. However, during the second (2021/22) and third (2022/23) epizootic waves, H5N1 was the dominant subtype. The rapid shift in dominance from H5N8 to H5N1 was likely driven by a combination of virological, immunological and/or host-related factors. In this study, we compared viral fitness and immunological responses in ducks, a key reservoir species, using dominant genotypes of H5N1 (genotype AB) and H5N8 (genotype A) from the second wave. While viral shedding dynamics were similar for both viruses, H5N8 was more pathogenic. Antigenic analysis of post-infection duck sera revealed that the haemagglutinin protein was antigenically similar across clade 2.3.4.4b H5 HPAIVs, but neuraminidase proteins displayed different patterns of cross-reactivity. We also modelled a scenario where ducks were pre-exposed to H5N1 (genotype C) or H5N8 (genotype A) from the first wave and subsequently challenged with either homologous or heterologous subtypes from the second wave (genotype AB or A). Despite the absence of seroconversion, pre-exposure to different subtypes resulted in varying clinical outcomes following challenge. These findings indicate that both viral and immunological factors likely played significant roles in the emergence and spread of H5Nx HPAIVs in wild bird populations.

INTRODUCTION

Influenza A viruses are subtyped according to the genetic and antigenic relatedness of the two surface glycoproteins, haemagglutinin (HA) and neuraminidase (NA). Currently, 17 different HA subtypes and 9 different NA subtypes of avian influenza virus (AIV) have been detected in wild birds. The HA protein can be broadly split into five clades, which form two groups: group one (clade 1, H8, H9, H12 and H19; clade 2, H1, H2, H5 and H6; clade 3, H11, H13 and H16) and group two (clade 1, H3, H4 and H14; clade 2, H7, H10 and H15) [1, 2]. A similar approach can be applied to the NA protein, which can be divided into two groups (group one, N1, N4, N8 and N5; group two, N6, N9, N7, N2 and N3) [2]. Due to the segmented nature of the AIV genome, which consists of eight genomic segments, different HA and NA combinations can arise via reassortment when two or

Received 23 April 2025; Accepted 06 August 2025; Published 01 September 2025

Author affiliations: [1]Influenza and Avian Virology Workgroup, Department of Virology, Animal and Plant Health Agency (APHA-Weybridge), Woodham Lane, Addlestone, Surrey KT15 3NB, UK; [2]Viral Pseudotype Unit, Medway School of Pharmacy, Universities of Kent and Greenwich, Chatham Maritime, Kent ME4 4TB, UK; [3]Department of Pathology and Animal Sciences, Animal and Plant Health Agency (APHA-Weybridge), Woodham Lane, Addlestone, Surrey KT15 3NB, UK; [4]Avian Influenza and Newcastle Disease Group, The Pirbright Institute, Ash Road, Pirbright, Woking, GU24 0NF, UK; [5]WOAH/FAO International Reference Laboratory for Avian Influenza, Animal and Plant Health Agency (APHA-Weybridge), Woodham Lane, Addlestone, Surrey KT15 3NB, UK.

***Correspondence:** Ashley C. Banyard, ashley.banyard@apha.gov.uk; Joe James, Joe.james@apha.gov.uk

Keywords: avian influenza virus (AIV); ducks; H5N1; H5N8; high pathogenicity avian influenza virus (HPAIV); immunity; pathogenicity.

Abbreviations: AIV, avian influenza virus; AUC, area under the curve; C, cloacal; dpc, days post-challenge; dpi, days post-infection; EFEs, embryonated fowl eggs; EID_{50}, 50% egg infectious dose; HA, haemagglutinin; HI, haemagglutination inhibition; HPAIV, high pathogenicity avian influenza virus; IC_{50}, inhibition concentration 50%; IHC, immunohistochemistry; IPs, infected poultry premises; IVPI, intravenous pathogenicity index; LM, Leibovitz L-15 Medium; LPAIV, low pathogenicity AIV; MBCS, multi-basic cleavage site; NA, neuraminidase; OD_{450}, OD at 450 nm; Op, oropharyngeal; pELLA, pseudotype-based enzyme-linked lectin assay; PV, pseudotype virus; PVNA, PV neutralization assay; REU, relative equivalent unit; RG, reverse genetics; RLU, relative luminescence per unit; RT-PCR, real-time PCR; SBCS, single-basic cleavage site; SD, sample diluent; SPF, specified pathogen free; VAERD, vaccine-associated enhanced respiratory disease; vRNA, viral RNA.

†Present address: Worldwide Influenza Centre, The Francis Crick Institute, 1 Midland Road, London NW1 1AT, UK.

Four supplementary figures and three supplementary tables are available with the online version of this article.

more AIVs co-infect the same cell. Reassortment of the internal gene segments can also generate new genotypes with different biological properties. Wild aquatic birds [mainly Anseriformes (waterfowl; ducks, geese, etc.) and Charadriiformes (shorebirds; gulls, waders, etc.)] serve as the reservoir for AIV in which nearly every combination of HA and NA subtypes can be found [2].

Since 2014, there have been repeated introductions of clade 2.3.4.4 H5Nx high pathogenicity avian influenza virus (HPAIV) of the A/goose/Guangdong/1/96 (gsGd) lineage into the European poultry sector, driven by the movements of wild bird species on migratory pathways [3]. The gsGd lineage epidemiology has been recently dominated by clade 2.3.4.4b HPAIVs, which continue to circulate in wild bird populations, and because of continual reassortment with other circulating AIVs, multiple different NA subtypes have emerged and established dominance in wild birds across Europe with resultant poultry incursions, including H5N8 (2014/15 and 2016/17), H5N6 (2017), H5N8 (2020/21) and H5N1 (2021/22 and 2022/23) [4–10].

During winter 2020/21 (wave 1), the magnitude of H5Nx epizootics escalated considerably [11]. In the UK and continental Europe, the first H5Nx epizootic wave (2020/21 autumn/winter) was the largest ever at the time. Wave 1 was dominated by a single subtype, H5N8, which was responsible for 96% of detections in UK poultry. A minor population of the H5N1 subtype was also circulating during this period, with H5N1 being responsible for 4% of detections in UK poultry [9, 10]. During wave 1, all H5N8 HPAIVs detected in the UK shared >98.1% sequence identity across all gene segments existing as a single genotype [European Reference Laboratory (EURL): genotype A; H5N8-W1 [12]]; similarly, all H5N1 detections also formed a single genotype (genotype C; H5N1-W1) [10].

At the end of the first wave (summer 2021) and at the start of the second wave (W2; 2021/22), H5N1 HPAIV emerged as the dominant subtype in the UK, with less than 1% of detections in wild birds and poultry being of other subtypes (H5N2 and H5N8), with only a single detection of H5N8 from a mute swan (*Cygnus olor*) in November 2021 [10, 13]. This initial H5N1 was genetically highly similar to H5N1-W1 which circulated as a minority subtype in the previous season (both were genotype C). Similarly, the single detection of H5N8 (H5N8-W2) was highly genetically related to the H5N8-W1 virus that had dominated previously (both were genotype A) [10].

As the second wave developed (autumn 2022) and transitioned into the third wave (2022/23), reassortment with other circulating AIVs contributed to increased genetic diversity within the H5N1 HPAIVs. However, importantly, little variation was observed in the HA gene between all H5N1 and H5N8 genotypes detected since wave 1. Four distinct H5N1 genotypes were detected more than once in poultry in the UK until the end of wave 3 (October 2023): genotypes AB, BB, C and AL [10, 14–18]. These genotypes have had varied detection frequencies, with the AB genotype (H5N1-W2) providing 50.9% of detections since it was first detected at the start of the second wave in the UK. This genotype of H5N1-W2 shared the PB1, NP, NA, MP and NS segments with H5N1-W1 [10, 19], but the PB2 and PA segments were most closely related to H5N3 AIVs from the first wave [10].

The rapid transition in dominance from H5N8 to H5N1 between wave 1 and wave 2 suggests (i) a potential phenotypic change in the virus or (ii) potential differential immune evasion mechanisms between the subtypes. Therefore, in this study, virological and host factors which may influence the continued evolution of H5Nx clade 2.3.4.4b HPAIVs in Anseriformes were investigated. Specifically, we investigated the relationship between the two epizootic seasons, where H5N8 dominated in wave 1 and H5N1 dominated in wave 2. Using virus isolates representative of those circulating in wave 2 of the epizootic in 2021/22 (H5N1-W2 and H5N8-W2), we compared *in vivo* fitness in ducks and interrogated antigenicity against HA and NA. The changing subtype dominance was modelled by exposing ducks to wave 1 viruses (H5N1-W1 and H5N8-W1) and then challenging with homologous or heterologous wave 2 viruses (H5N1-W2 or H5N8-W2).

METHODS

Viruses and propagation

Six AIV strains were used in this study (Table S1, available in the online Supplementary Material). Two viruses represented the first wave epizootic (October 2020–September 2021): A/chicken/England/030786/2020 (H5N8, genotype A; H5N8-W1; GISAID: EPI_ISL_17212363) and A/mute swan/England/234255/2020 (H5N1, genotype C; H5N1-W1; GISAID: EPI_ISL_766876). De-engineered versions of both viruses were generated by substituting the multi-basic cleavage site (MBCS) with a single-basic cleavage site (SBCS) via reverse genetics (RG) (described previously [20]), resulting in SB-H5N8-W1 and SB-H5N1-W1.

For *in vivo* challenge studies, two HPAIVs from the second wave epizootic (October 2021–September 2022) were used: A/chicken/Scotland/054477/2021 (H5N1, genotype AB; H5N1-W2; GISAID: EPI_ISL_9012696) and A/mute swan/England/298902/2021 (H5N8, genotype A; H5N8-W2; GISAID: EPI_ISL_13369742).

All viruses were propagated in 9-day-old specified pathogen free (SPF) embryonated fowl eggs (EFEs) and titrated in EFEs to determine the 50% egg infectious dose (EID_{50}), as previously described [21]. The full genomes of all viruses used in this study were sequenced, as previously described [10], to confirm that no AA polymorphisms had emerged following passage, when compared with the original sequence.

Animals

High health status Pekin ducks (*Anas platyrhynchos*) (Cherry Valley hybrid; Cherry Valley Farms Ltd., UK) of mixed sex (52% female; 48% male, total 36) were obtained at 1 day old and reared until 3 weeks of age at the time of infection. Ducks were acclimatized for 7 days prior to the first procedures which included swabbing [oropharyngeal (Op) and cloacal (C)] and bleeding from a superficial vein prior to inoculation. These samples were tested using an M-gene reverse transcription real-time PCR (RT-PCR) [22] and serological testing [21] using the ID Screen® Influenza A Antibody Competition Multi-species ELISA kit (IDVet, France). For the intravenous pathogenicity index (IVPI) test, white Leghorn SPF chickens (*Gallus gallus domesticus*) (Valo, Germany) were reared at APHA until 4 weeks of age.

Experimental design

The statutory IVPI test was performed on de-engineered viruses (SB-H5N1-W1 and SB-H5N8-W1) as per WOAH guidelines [21]. Virus isolates were diluted 1:10 in isotonic saline, and 100 µl (10^8 EID_{50}/bird) was administered intravenously into the wing vein of 4-week-old chickens (n=10).

For infection and prior-immunity studies, two groups of immunologically naïve 3-week-old ducks (n=6/group) were inoculated via the ocular-nasal route with 10^5 EID_{50} of either H5N1-W2 or H5N8-W2 in 100 µl of PBS (Fig. S1). Op and C swabs were collected daily from 1 to 14 days post-infection (dpi). Birds were euthanized upon reaching humane endpoints or at 14 dpi, when blood was collected via cardiac puncture under terminal anaesthesia.

For prior-exposure studies, two groups of ducks (n=12/group) were inoculated oronasally with 10^7 EID_{50} of SB-H5N1-W1 (N1) or SB-H5N8-W1 (N8) (Fig. S1). At 13 dpi, blood was collected from all birds, after which each group was split into two (n=6/group) and challenged oronasally with 10^5 EID_{50} of either H5N1-W2 or H5N8-W2. This formed four groups: N1/N1 and N8/N1 (H5N1-W2 challenge) and N1/N8 and N8/N8 (H5N8-W2 challenge). From 1–14 days post-challenge (dpc), Op and C swabs were collected daily. Birds were euthanized at humane endpoints or at 14 dpc (28 dpi total), when terminal blood collection was undertaken.

Clinical scoring and monitoring

Birds were observed and scored against a defined clinical score sheet (Table S2) twice a day (morning and afternoon). Following the development of clinical disease, birds were additionally observed at a third timepoint (evening). Birds were terminated whenever clinical endpoints were reached (cumulative score >7; Table S2). For ethical reasons, any birds housed singularly, due to euthanasia or death of others within the group, were also euthanized.

Clinical sample collection, processing and immunohistochemistry

Swabs were individually cut and placed into 1 ml of Leibovitz L-15 Medium (LM; Gibco [23]), and the supernatant was used for RNA extraction or stored at −80 °C until further use. During the post-mortem examination, ~50 mg of tissue from selected organs was collected into 1 ml LM and mechanically homogenized, with the clarified homogenate being used for RNA extraction. In addition, tissues were harvested from all major organs and fixed in 10% (v/v) neutral buffered formalin for a minimum period of 5 days before being embedded in paraffin. Four-micron thick serial sections were stained with haematoxylin and eosin, and for immunohistochemistry (IHC), using a mouse monoclonal anti-influenza A nucleoprotein antibody (Statens Serum Institute, Copenhagen, Denmark) as described previously [23]. The overall distribution of virus-specific staining in each tissue was assessed using a semi-quantitative scoring system (0=no staining, 1=minimal, 2=mild, 3=moderate and 4=widespread staining) modified from Löndt *et al.* [24]. Specificity of immunolabelling was assessed in positive control sections by replacing the primary antibody with a matching mouse IgG isotype; no non-specific cross-linking was observed.

Environmental sample collection and processing

Following infection with HPAIV at 14 dpi, environmental samples of drinking water and pond water were collected on alternate days from each duck pen. Air samples were collected, as described previously [23, 25], from the environment of ducks infected with either H5N1-W2 or H5N8-W2. Viral RNA (vRNA) was extracted directly from water samples and from supernatants of gelatine air filters dissolved in LM as described previously [25].

RNA extraction and AIV reverse transcription RT-PCR

vRNA was extracted from LM obtained from swabs, tissues, feathers and environmental samples using the MagMAX™ CORE Nucleic Acid Purification Kit (Thermo Fisher Scientific™) and the robotic Mechanical Lysis Module (KingFisher Flex System; Life Technologies), according to the manufacturer's instructions. Extracted RNA was tested by the M-gene RT-PCR using the primers and probes as previously described [22]. A tenfold dilution series of RNA extracted from a stock of H5N1-W2 HPAIV with a known EID_{50} titre was used to construct a standard curve, and Ct values were converted to relative equivalent unit (REU)

as previously described [23, 26]. RT-PCR Ct values <36 (>$10^{1.794}$ REU) were considered as AIV positive, and Ct values ≥36 (≤$10^{1.794}$ REU) were considered negative.

Serum processing and haemagglutination inhibition assays

Whole blood samples were centrifuged for 5 min at 2,000 r.p.m. to separate the serum from the clot. Sera were incubated at 56 °C for 30 min to inactivate complement. The duck sera were pre-absorbed by adding packed chicken red blood cells and incubated at 4 °C overnight to prevent non-specific agglutination [21]. Haemagglutination inhibition (HI) assays were conducted using different antigens initiated at four HA units. Reciprocal HI titres of >1/16 were considered seropositive as defined internationally [21]. All sera were also tested by the ID Screen® Influenza A Antibody Competition Multi-species ELISA kit (IDVET, France) according to the manufacturer's instructions.

Influenza pseudotype virus generation

Lentiviral pseudotype viruses (PVs) containing H5Nx glycoproteins were generated for H5N1-W2 (genotype C) (A/chicken/England/053052/2021), H5N1-W2 (genotype AB) (A/chicken/Scotland/054477/2021) and H5N8-W1 (genotype A) (A/chicken/England/030786/2020) (Table S1). Existing PVs were used for H5N8-14 (A/gyrfalcon/Washington/41088-6/2014) [27]. The HA and NA genes were subcloned from pHW2000 into pCAGGS using a directional *NotI-XhoI* restriction digest strategy. PVs were generated as previously described [27], employing p8.91 gag-pol vector as retroviral core. PV titres were assessed by transduction of HEK293T/17 cells as previously described [27], employing the Bright-Glo assay system (Promega) and read as relative luminescence per unit (RLU).

PV neutralization assay

For PV neutralization assay (PVNA), serum was first prediluted 1:100 and tested in duplicate against H5 PVs. Chicken reference serum raised against A/chicken/Scotland/59 (H5N1) (product code: RAA7002) and A/duck/England/036254/14 (H5N8) (product code: RBB6425) (APHA Scientific, UK). Briefly, sera were serially diluted 2-fold in a 96-well white plate, and 10^6 RLU of PV was added to each well. The plate was incubated for 1 h at 37 °C to allow binding of the antibody to the antigen. Next, 10^4 HEK293T/17 cells were added to each well. PV-only and cell-only controls were included in the plate to represent the 0% and 100% neutralization of the PV. The plate was incubated for 48 h at 37 °C at 5% CO_2 before reading. Data were normalized and plotted on a neutralization percentage scale, and the reciprocal of the serum dilution which induces 50% neutralization or IC_{50} was calculated as previously described [28].

Pseudotype-based enzyme-linked lectin assay

To investigate NA-reactive antibodies, HA and NA PVs were employed. H5Nx PVs were generated and titrated via the pseudotype-based enzyme-linked lectin assay (pELLA) method as previously described [29]. OD at 450 nm (OD_{450}) was determined using the Multiskan™ FC microplate photometer with SkanIt™ software for data analysis. Readings were normalized to 100% and 0% OD_{450}, and the dilution that resulted in 90% OD_{450} was selected for inhibition assays. The inhibition of NA activity by serum samples was evaluated via pELLA. Serum was tested in duplicate against H5N1 and H5N8 PVs. The sera were pre-diluted 1:10 prior to the inhibition assay. Sera were then diluted 1:100 and then serially diluted twofold in 50 µl sample diluent (SD). Fifty microlitres of these dilutions were then transferred to fetuin-coated plates containing 50 µl of SD to all wells, excluding SD-only and PV-only controls, representing 100% and 0% inhibition, respectively. Fifty microlitres of the H5Nx PV 90% OD_{450} as determined in the titration were then transferred to all wells of the fetuin-coated plate except for SD-only control. All other steps were followed as per NA PV titration via the pELLA. The IC_{50} was calculated as the inverse dilution of serum that resulted in 50% inhibition of NA activity as determined via GraphPad Prism.

Statistical analysis

Area under the curve (AUC) analysis of individual bird shedding profiles was performed using GraphPad Prism v8, with values expressed as REU. Birds that did not shed were assigned an AUC value of 0 REU. Mean AUC values were calculated and compared for statistical significance using one-way ANOVA with multiple comparisons in GraphPad Prism v8. Statistical significance was defined as $P<0.05$. For pELLA analysis, mean and SD medians were derived for each data point based on two replicates per dilution. Kaplan–Meier survival curves were evaluated using the Gehan–Breslow–Wilcoxon test in GraphPad Prism v8.

RESULTS

Comparative fitness in ducks of 2.3.4.4b H5N1 and H5N8 HPAIV circulating during the second epizootic wave

The *in vivo* fitness of H5N1-W2, a HPAIV representative of the dominant genotype (AB) during the second epizootic wave, was compared with H5N8-W2 (genotype A) from the same period (Fig. S1). Inoculation of naïve ducks with either virus resulted in productive infection, with high vRNA shedding from the Op cavity (Fig. 1a, b). Both viruses showed similar shedding profiles;

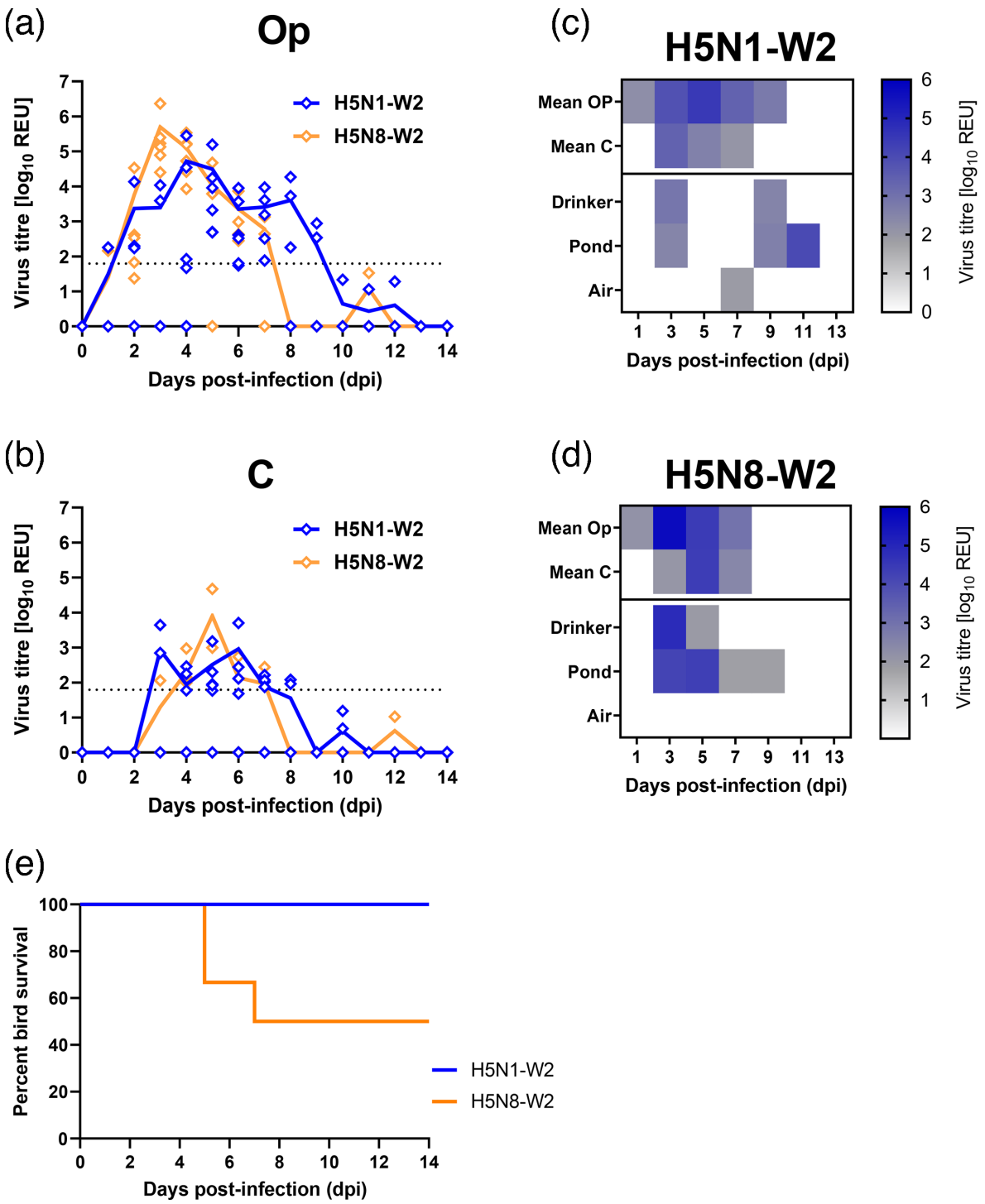

Fig. 1. Virus shedding, environmental contamination and survival from ducks infected with H5N1-W2 and H5N8-W2 HPAIVs. (a, b) Viral shedding measured from swab samples collected from the Op (a) and C (b) cavities of naïve ducks following infection with H5N1-W2 (blue) or H5N8-W2 (orange) HPAIV. vRNA titres were quantified by M-gene RT-PCR and expressed as $\log_{10}$ REU. Individual data points are shown, with coloured lines indicating the group mean. The dotted horizontal line represents the diagnostic Ct threshold (Ct 36.00; $10^{1.794}$ REU) for M-gene RT-PCR positivity. (c, d) Heatmaps representing the quantification of vRNA ($\log_{10}$ REU) for H5N1-W2 (c) and H5N8-W2 (d). The top two rows of each panel correspond to the mean shedding from Op and C swabs, as shown in panels (a) and (b). Environmental samples (drinking water, pond water and air) were collected on alternate days. Heatmap shading indicates vRNA detection: white denotes no Ct value, grey represents samples below the diagnostic threshold ($10^{1.794}$ REU) and blue indicates positive samples. (e) Percentage survival of ducks over a 14-day period post-infection (dpi) with H5N1-W2 (blue) or H5N8-W2 (orange) HPAIV.

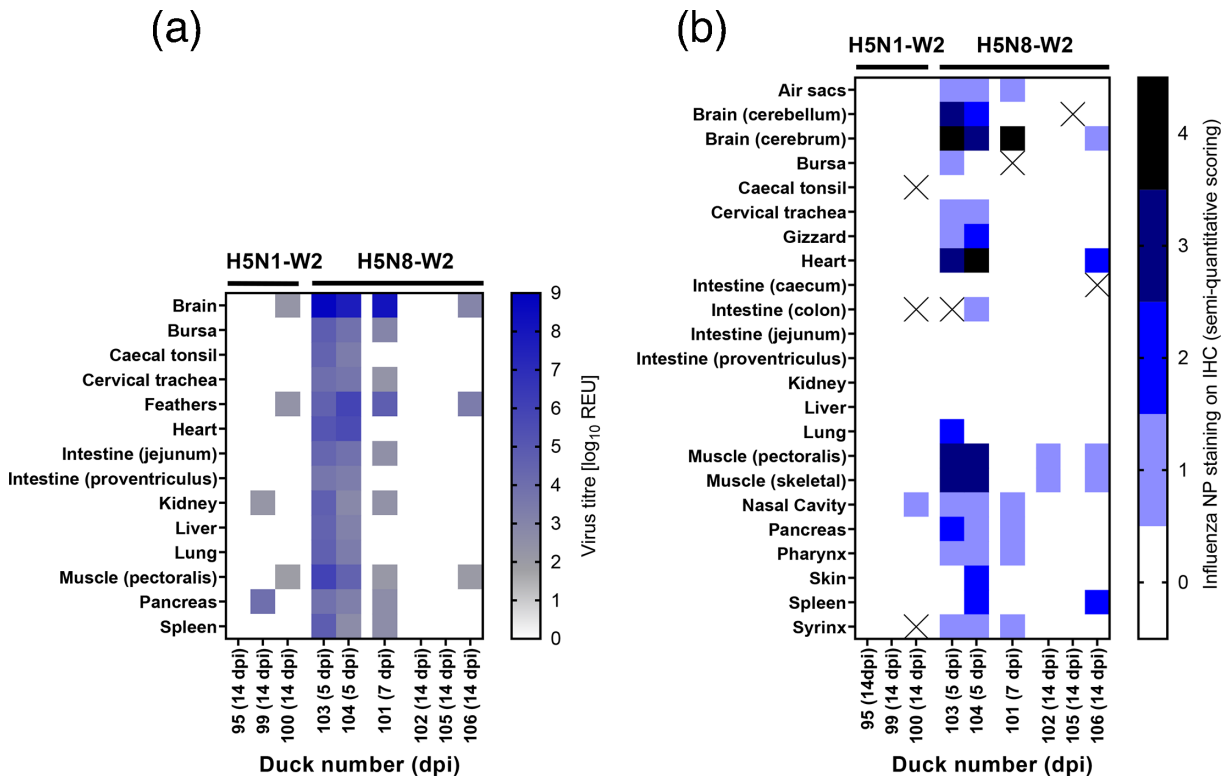

Fig. 2. Virus distribution in tissues of ducks infected with H5N1-W2 or H5N8-W2 HPAIV. (a) Quantification of vRNA in tissue samples collected from nine ducks infected with H5N1-W2 (*n*=3) or H5N8-W2 (*n*=6) HPAIV. Ducks were euthanized due to severe clinical signs or culled at the study endpoint (14 dpi). vRNA levels were measured by M-gene RT-PCR and expressed as $\log_{10}$ REU, represented as a heatmap. Samples with Ct values below the diagnostic threshold ($10^{1.794}$ REU) are shown in grey, positive samples in blue and samples with no detectable Ct value in white. (b) Semi-quantitative scoring of anti-NP staining intensities and distribution in IHC analysis of tissues (lower to higher intensities, 0–4), while the 'X' indicates that no sample was available for IHC.

however, H5N8-W2 exhibited a higher mean peak shedding on 3 dpi, while H5N1-W2 peaked later, at 4 dpi, with a lower mean titre. Notably, H5N1-W2-infected ducks shed vRNA for a longer duration. C shedding was broadly similar, though a higher proportion of ducks shed vRNA after H5N1-W2 infection (H5N1-W2, 100%; H5N8-W2, 50%). However, AUC analysis showed no significant difference between H5N1-W2 and H5N8-W2 in overall Op or C shedding (Op, *P*-value 0.229; C: *P*-value 0.477). Environmental contamination was found in the drinking and pond water with vRNA detected from 3 dpi in both groups, but less consistently in the H5N8-W2 group (Fig. 1c, d). vRNA was present in water on 3, 9 and 11 dpi for H5N1-W2 and on 3 and 5 dpi for H5N8-W2. Airborne vRNA was only detected at 7 dpi in the H5N1-W2 group.

Clinical outcomes in ducks with H5N1 and H5N8 HPAIV circulating during the second epizootic wave

All ducks infected with H5N1-W2 survived until the end of the study (14 dpi), whereas only 50% of those infected with H5N8-W2 survived (two ducks were euthanized at 5 dpi and one at 7 dpi) (Fig. 1e). H5N1-W2 infection induced fewer clinical signs, with a total clinical score of 8, compared with a score of 90 in the H5N8-W2 group (Table S2). Ducks infected with H5N8-W2 also exhibited more severe neurological signs, including tremors (seven counts), torticollis (one count) and seizures (one count) (Table S2, Fig. S2A and B).

A post-mortem examination was conducted on three H5N1-W2-infected ducks and six H5N8-W2-infected ducks. As no H5N1-W2 ducks required culling, comparisons between groups are only possible at 14 dpi. Among the three H5N8-W2-infected ducks culled between 5 and 7 dpi (ducks 101, 103 and 104), vRNA was detected in all sampled tissues from ducks 103 and 104 (5 dpi), while duck 101 tested negative in the heart, lung, caecal tonsil, proventriculus and liver (Fig. 2a). Notably, all three showed high vRNA levels in brain and feather samples, with mean titres of $10^{8.41}$ and $10^{5.48}$ REU, respectively. High REU titres in the brain are consistent with the increased neurological impact of the H5N8-W2-infected ducks. The H5N8-W2 group had 11 clinical counts, including 7 of tremors, compared with only a single observation of neurological disease signs in the H5N1-W2-infected group (Table S2). Of the six surviving ducks culled at 14 dpi, vRNA was detected only sporadically, and at a low level, in the brain,

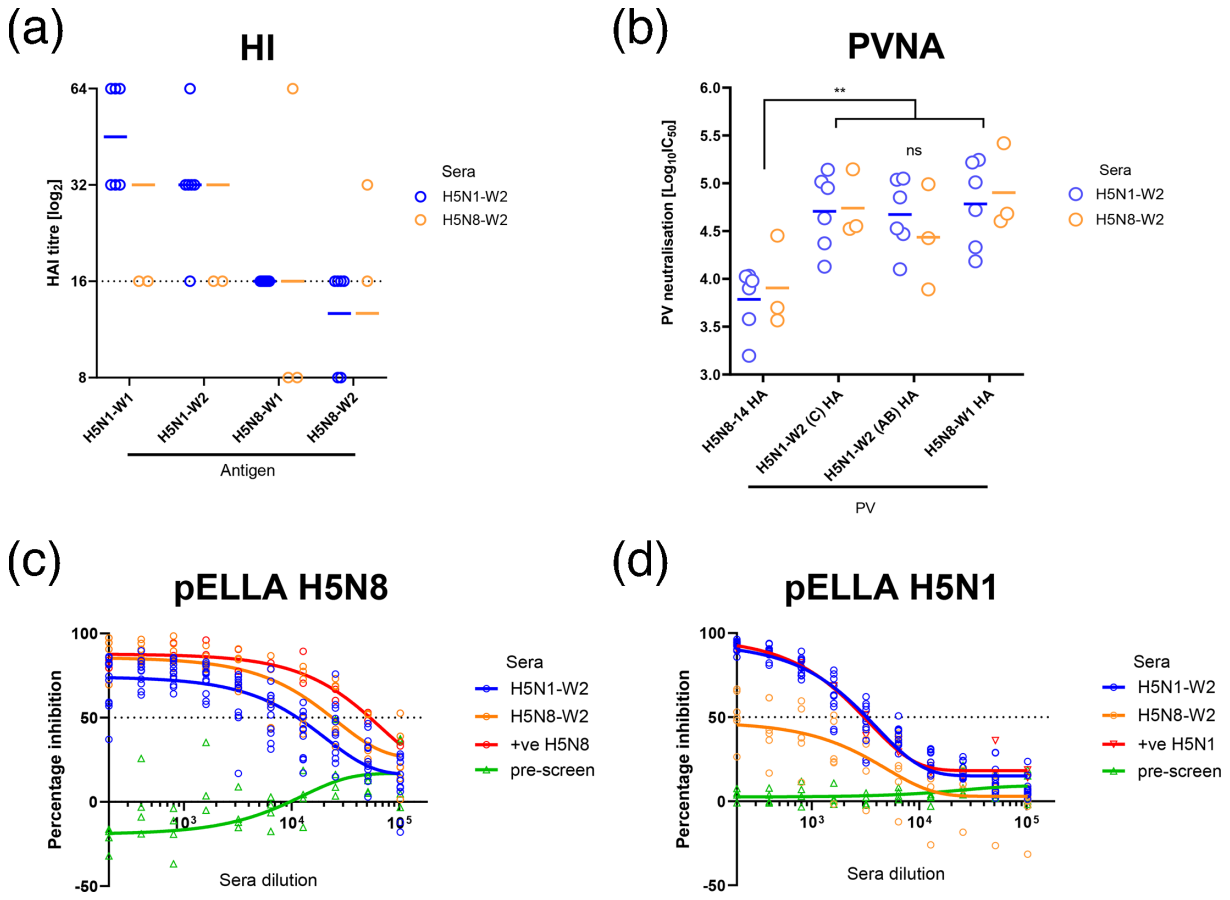

Fig. 3. Serological responses and antigenic characterization of H5N1-W2 and H5N8-W2. Serological responses using sera collected from ducks at 14 dpi infected with H5N1-W2 AB (blue) or H5N8-W2 A (orange); sera assessed using HI (a) or lentiviral PVs containing H5Nx influenza virus HA or HA and NA glycoproteins (b–d). Coloured horizontal bars indicate geometric mean titres, while the dotted line indicates the diagnostic threshold for positivity (1:16). (a) HI using sera from ducks infected with H5N1-W2 or H5N8-W2, against antigens with homologous or heterologous NAs from 2021 or 2020. (b) PV neutralization titres (IC_{50}) using PVs containing H5 HA only evaluated against individual sera from H5N1-W2 or H5N8-W2 infected ducks. (c, d) Sera assessed by pELLA using PVs containing HA and NA glycoproteins tested against pre-infection (green), homologous subtype positive control (red), H5N1-W2 (blue) or H5N8-W2 (orange) tested against post-infection sera from H5N1-W2 or H5N8-W2-infected ducks.

muscle or feathers in one H5N8-W2-infected duck (106) and one H5N1-W2-infected duck (100). Another H5N1-W2-infected duck (99) had detectable vRNA only in the pancreas and kidney.

IHC analyses were also performed on tissues from these birds. At 5 dpi, brain samples from H5N8-W2 ducks showed acute non-suppurative encephalitis with extensive viral antigen in neurons (Figs 2b and S3A and B). By 14 dpi, only minimal multi-focal gliosis and sparse antigen were observed, indicating viral clearance. In the heart, acute myocardial degeneration with monocytic infiltration and abundant antigen was seen at 4–5 dpi. The pectoral muscle displayed mild non-suppurative myositis with variable antigen labelling. By 14 dpi, lesions in both the heart and muscle had resolved to mild chronic inflammation and lymphoid hyperplasia. Minimal antigen remained in macrophages within lymphoid aggregates, suggesting resolution of active viral replication. This was consistent with the reduction in vRNA titres detected in the tissues by 14 dpi.

Serological responses and antigenic cross-reactivity between H5N1 and H5N8 subtypes

Serological responses following infection with H5N1-W2 and H5N8-W2 were compared. All surviving infected ducks (n=6 H5N1-W2; n=3 H5N8-W2) were positive by NP ELISA (data not shown) and seroconverted against the H5N1-W2 antigens in the HI assay, at 14 dpi (Fig. 3a). Lower, but not statistically significant, HI titres were detected when sera from both infections were tested against the H5N8-W2 compared with the H5N1-W2 antigen. Serum from two birds in the H5N1-W2 group and one bird in the H5N8-W2 group failed to seroconvert against H5N8-W2 antigen. No statistically significant differences were observed between reactivity of viruses with sera of the same subtype from wave 2 or wave 1 (H5N1-W2 compared with H5N1-W1 and the reciprocal) (Fig. 3a). To assess HA-specific antibody responses, PVs displaying only the HA proteins of clade 2.3.4.4b H5N1

and H5N8 strains were used, alongside an earlier clade 2.3.4.4c H5 (H5N8-14) PV as a reference. Although both sera neutralized H5N8-14 PV, IC_{50} values were significantly lower than those for the more recent H5 PVs (Fig. 3b). No significant differences in neutralization titres were found between the 2.3.4.4b H5 PVs using either serum (Fig. 3b). To evaluate NA-specific responses, pELLA was performed using PVs containing both HA and NA. H5N1 and H5N8 antisera inhibited their homologous PVs with IC_{50} values of $10^{3.68}$ and $10^{4.89}$, respectively (Fig. 3c, d). Pre-infection sera showed no cross-reactivity to either PV. Post-infection sera from both groups (H5N1-W2 and H5N8-W2 sera) robustly inhibited H5N8 PV (IC_{50} $10^{4.28}$ for H5N1-W2 and $10^{4.58}$ for H5N8-W2). However, H5N1-W2 sera only strongly inhibited the H5N1 PV (IC_{50} $10^{3.68}$); H5N8-W2 sera showed a low ability to inhibit H5N1 PV, with inhibition curves failing to reach 50% (Fig. 3c, d).

H5N1 and H5N8 clade 2.3.4.4b H5Nx HPAIV without MBCSs have reduced pathogenicity yet are able to productively infect chickens

To replicate the natural exposure scenario observed between 2020 and 2022, we next modelled sequential infection in wild birds, with initial exposure to wave 1 viruses (H5N1-W1 or H5N8-W1) followed by re-infection with wave 2 viruses (H5N1-W2 or H5N8-W2). To ensure survival after primary exposure, we attempted to reduce the pathogenicity of the viruses while retaining the antigenicity. Therefore, we used RG to generate low pathogenic variants (SB-H5N1-W1 and SB-H5N8-W1) by replacing the MBCS with an SBCS (Fig. S4C). Both SB viruses reached high titres in EFEs (SB-H5N1-W1, $10^{10.50}$ EID_{50}/ml; SB-H5N8-W1, $10^{10.00}$ EID_{50}/ml), comparable to their WT HPAIV counterparts (H5N1-W1, $10^{9.85}$; H5N8-W1, $10^{9.48}$). IVPI testing confirmed a low pathogenic phenotype (SB-H5N1-W1, 0.15; SB-H5N8-W1, 0.0), yet all surviving birds in the SB-H5N8-W1 group seroconverted by 10 dpi, and 7/9 birds seroconverted in the SB-H5N1-W1 group, confirmed by homologous HI titres (Fig. S4A). One mortality occurred in the IVPI at 6 dpi in the SB-H5N1-W1 group. vRNA was detected in multiple tissues and swabs from this animal (Fig. S4B), but sequencing confirmed retention of the engineered SBCS (Fig. S4C).

The effect of homo- and hetero-subtypic prior exposure on shedding dynamics of the H5N1 and H5N8 clade 2.3.4.4b HPAIV

We next inoculated ducks, as surrogates for wild aquatic birds, with SB-H5N1-W1 or SB-H5N8-W1 viruses, followed by homologous (N1/N1, N8/N8) or heterologous (N1/N8, N8/N1) HPAIV challenge with H5N1-W2 or H5N8-W2 (Fig. S1). Following inoculation with the de-engineered viruses, vRNA was detected in only 3 of 12 ducks in the SB-H5N1-W1 groups (N1/N1, N1/N8), all below the positive threshold; no vRNA was detected in the SB-H5N8-W1 groups (N8/N8, N8/N1). No clinical signs were observed, and all ducks were seronegative by HI at 13 dpi [HI titres<2, 1/22 ducks were borderline by NP ELISA, while the remaining 21 ducks were negative by NP ELISA (data not shown)]. Following the challenge with H5N1-W2, ducks previously exposed to SB-H5N1-W1 (N1/N1) exhibited a 4-day delay in vRNA detection in Op swabs compared with naïve controls (Fig. 4a). A similar delay was observed in C swabs (Fig. 4e). Despite this, both groups reached comparable peak vRNA levels, with Op ~2 log_{10} higher than C shedding (Fig. 4a, e). Total shedding (AUC) did not differ significantly between groups (Op, *P*-value 0.9991; C, *P*-value 0.9941). vRNA was detected in water from the N1/N1 group from 7 to 11 dpi; a 4-day delay compared with the naïve H5N1-W2 group (Fig. 5a vs. Fig. 1c). In the heterologous challenge (N1/N8), prior SB-H5N1-W1 exposure delayed shedding onset by 2 days relative to naïve H5N8-W2-infected ducks, though both groups peaked at 3 dpi (Fig. 4b). Water contamination was detected at 3 dpi in both groups but persisted longer (until 9 dpi) in the naïve (H5N8-W2) group (Figs 1d and 5d). The delay in shedding onset in the N1/N1 and N1/N8 groups was most apparent early in infection (Fig. 4a, b).

In contrast, prior SB-H5N8-W1 exposure had minimal impact on vRNA shedding. Ducks subsequently challenged with H5N1-W2 (N8/N1) or H5N8-W2 (N8/N8) showed similar vRNA shedding profiles to naïve controls (Fig. 4c, d, g and h). Environmental contamination was also similar (Fig. 5b, c). Water from the N8/N1 group showed comparable levels to naïve H5N1-W2-infected ducks, although shedding was more prolonged in the naïve H5N1-W2 ducks (Figs 1c and 5b). For the N8/N8 group, vRNA was detected in water, but sample collection ceased at 5 dpi due to mortality in all ducks, limiting comparison (Figs 1d, 5c and 6b).

The effect of homo- and hetero-subtypic prior exposure on disease outcomes and pathogenesis

In the H5N1-W1 pre-exposed ducks, no mortality was observed following challenge with H5N1-W2 (N1/N1), consistent with the survival of naïve H5N1-W2-infected ducks (Fig. 6a). Both groups also exhibited reduced clinical severity compared with ducks exposed to or infected with H5N8 viruses (Fig. S2). In contrast, prior exposure to H5N1-W1 reduced mortality and clinical signs following H5N8-W2 challenge (N1/N8) compared with the naïve group, but not statistically significantly (Fig. 6b, Table S2).

However, in the N8 pre-exposed group, homologous H5N8 re-challenge (N8/N8) resulted in statistically significantly higher mortality (*P*=0.0139, Gehan–Breslow–Wilcoxon test) and greater clinical severity compared with the naïve H5N8 group (Figs 6b and S2B, D), with 100% of ducks culled due to severe disease (two at 4 dpc, four at 5 dpc), compared with 50% in the naïve group (two at 5 dpc, one at 7 dpc) (Fig. 6). Prior H5N8-W1 exposure also increased mortality upon H5N1-W2 challenge (N8/N1).

Tissue tropism was assessed only in ducks that succumbed to infection. vRNA was detected in multiple tissues from N1/N8, N8/N1 and N8/N8 groups, with the highest titres in brain samples (Fig. 7a). High vRNA levels were also found in feathers, cervical

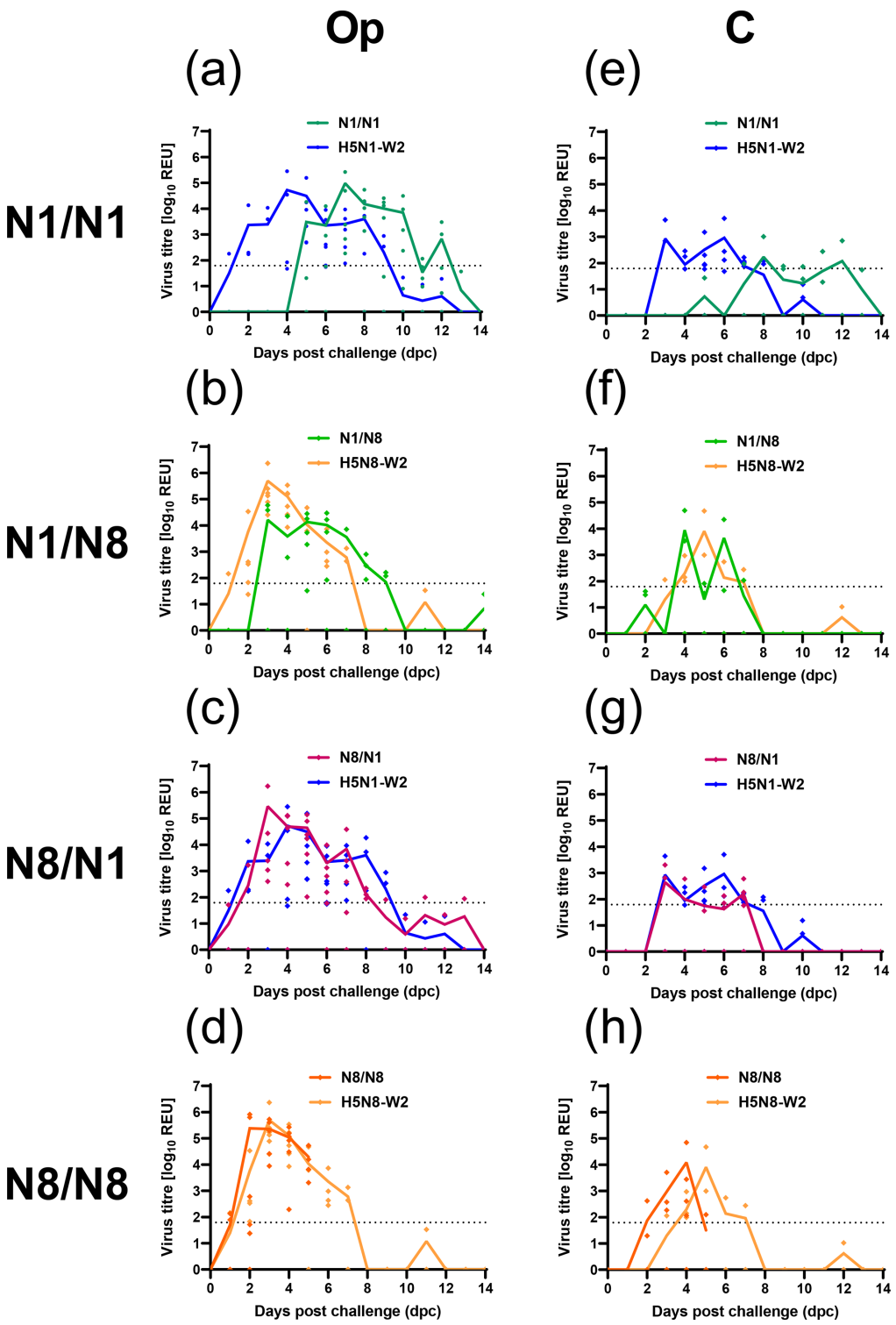

Fig. 4. Virus shedding from ducks infected with H5N1-W2 and H5N8-W2 HPAIV with prior exposure to de-engineered H5N1-W1 and H5N8-W1 AIVs. Groups of ducks were initially inoculated with either H5N1-W1 (N1) or H5N8-W1 (N8) de-engineered AIVs. After 14 dpi, the groups were divided, and ducks were challenged with either HPAIV H5N1-W2 or H5N8-W2. This resulted in homologous (N1/N1 (a, e) and N8/N8 (d, h), or heterologous (N1/N8 (b, f) and N8/N1 (c, g) subtype combinations. Shedding was measured from Op (a–d) and C (e–h) swabs following challenge. Shedding from naïve birds is also shown for reference. vRNA titres were determined by M-gene RT-PCR and expressed as $\log_{10}$ REU. Individual shedding values are shown by coloured symbols, with group mean shedding shown by continuous coloured lines. Dotted horizontal lines indicate the M-gene RT-PCR-positive cut-off ($10^{1.794}$ REU).

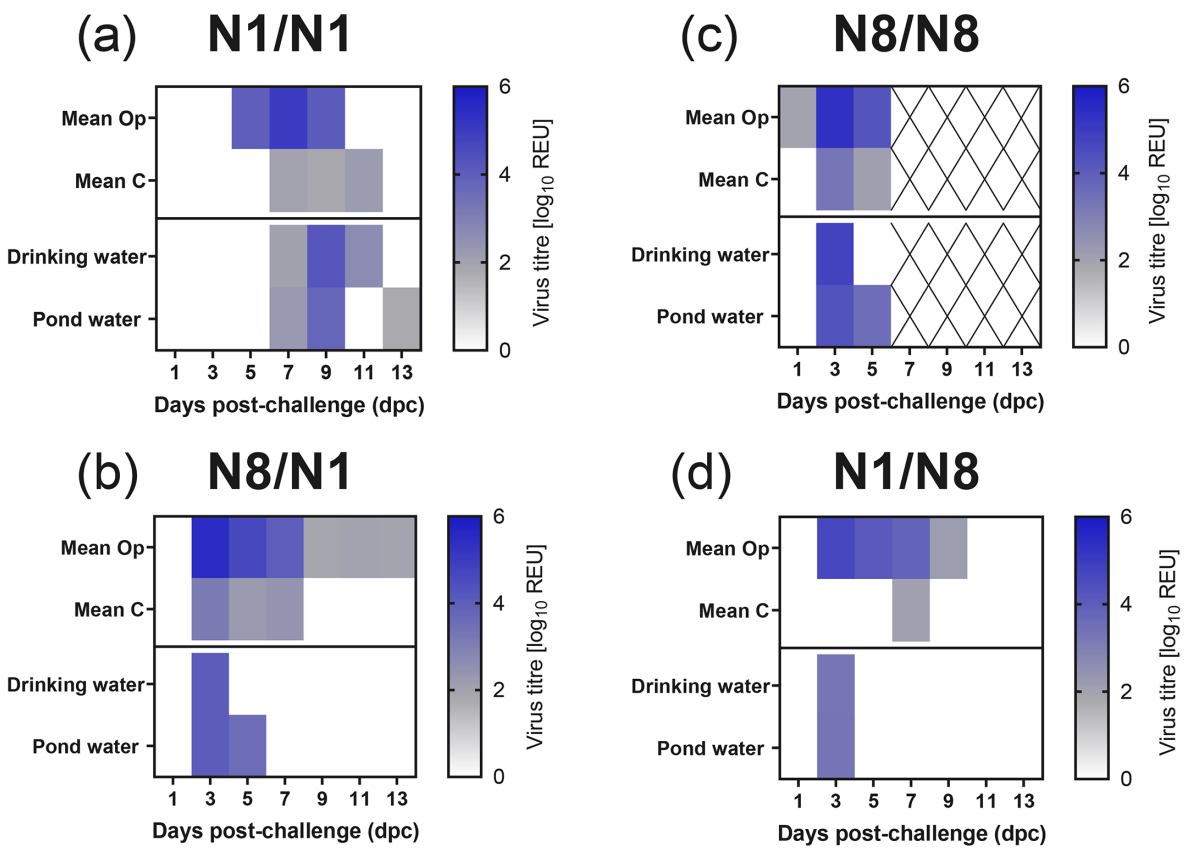

Fig. 5. Viral environmental contamination from ducks challenged with H5N1-W2 and H5N8-W2 HPAIV, following prior exposure to de-engineered H5N1-W1 and H5N8-W1 AIVs. Environmental specimens were collected between 1 and 13 dpc from drinking and pond waters of ducks. The ducks had been challenged with HPAIV H5N1-W2 or H5N8-W2 but had previously been exposed to homologous [N1/N1 (a) and N8/N8 (c)] or heterologous [N1/N8 (d) and N8/N1 (b)] subtype of de-engineered H5N1-W1 or H5N8-W1 AIVs. vRNA titres were determined by the M-gene RT-PCR. Samples were shown as a heatmap with no Ct in white, below the diagnostic cut-off ($10^{1.794}$ REU) shown in grey and positive samples in blue. 'X' indicates that no sample was collected at the specific time point. The top two rows on all graphs represent the mean Op and C shedding titres from all birds.

trachea and intestines of N1/N8 and N8/N8 ducks. In contrast, no vRNA was detected in tissues from the N8/N1 bird, which also showed lower IHC scores across tissues compared with H5N8-W2-challenged birds (Fig. 7a, b). Histopathological lesions and immunolabelling in N1/N8 and N8/N8 ducks mirrored those in naïve H5N8-W2-infected birds (Figs S3C, D). Moderate multifocal non-suppurative encephalitis with gliosis and perivascular cuffing was observed in the brain, with abundant neuronal antigen. Acute myocardial degeneration and necrosis with co-localized viral antigen were evident in the heart and pectoral muscle (Fig. 7b). In contrast, N8/N1 ducks displayed minimal lesions, and no tissue samples were available from the N1/N1 group.

DISCUSSION

During the H5Nx clade 2.3.4.4b panzootic, a notable shift in NA subtype dominance occurred in the UK and continental Europe. In the 2020–2021 season (wave 1), H5N8 predominated, with 26 infected poultry premises (IPs) and 285 wild bird cases reported in the UK, compared with only 2 IPs and 18 wild bird detections of H5N1. However, by 2021–2022 (wave 2), H5N1 became dominant, with 157 IPs and 1,629 wild bird detections, while H5N8 was detected only once, in a single mute swan (*C. olor*), with no poultry cases [9, 10]. For a particular H5Nx virus to emerge and achieve epidemiological dominance, it must replicate to sufficiently high levels within a specific host species to enable shedding at titres capable of facilitating onward transmission to further susceptible hosts. The emergence and persistence of novel subtypes and genotypes are likely influenced by a degree of stochasticity, as some infected hosts may represent ecological or epidemiological dead ends. Additionally, genetic bottlenecks are likely to occur at breeding sites and during migratory events. Consequently, successful infection and transmission must occur with sufficient frequency to enable sustained circulation at the population level. From both virological and host-related

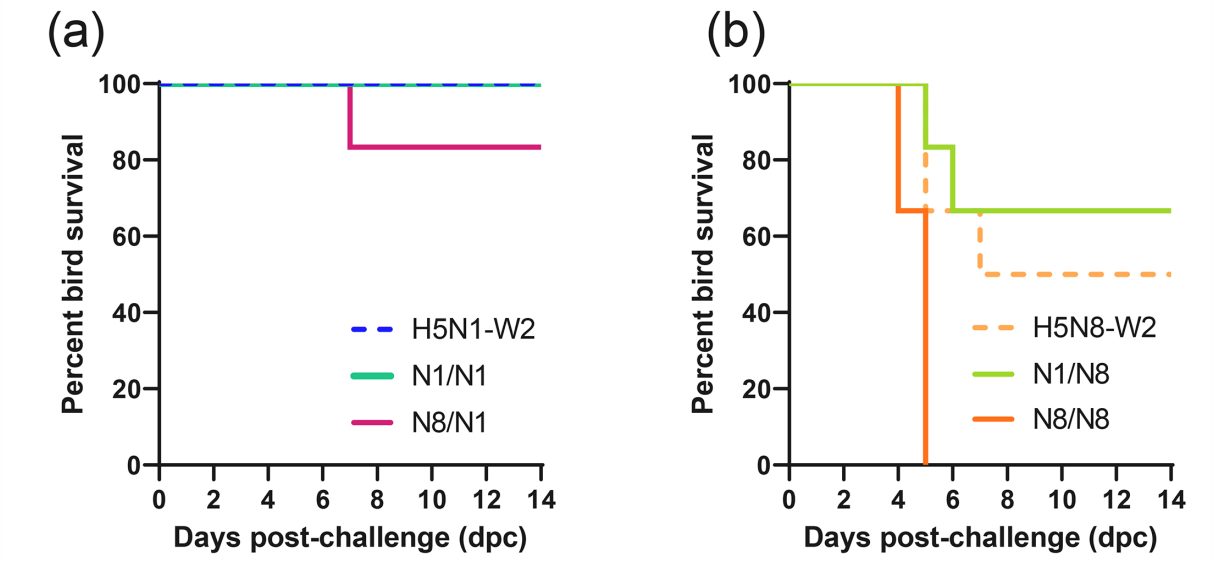

Fig. 6. Survival of ducks challenged with H5N1-W2 and H5N8-W2 HPAIV, with or without prior exposure to de-engineered H5N1-W1 and H5N8-W1 AIVs. Percentage survival of ducks until 14 dpc following challenge with (a) HPAIV H5N1-W2 or (b) H5N8-W2 with no prior exposure (hashed lines), or ducks which had previously been exposed to (solid lines) homologous (N1/N1 and N8/N8) or heterologous (N1/N8 and N8/N1) subtypes of de-engineered H5N1-W1 or H5N8-W1 AIVs.

perspectives, the rapid displacement of H5N8 by H5N1 may reflect (i) alterations in viral virulence, infectivity or tissue tropism; (ii) differences in the capacity to evade host immunity; or (iii) a combination of these factors.

To assess virological fitness, representative H5N1 and H5N8 viruses from wave 2 were compared *in vivo*. Both H5N1-W2 and H5N8-W2 established productive infections, with all ducks shedding virus and seroconverting. Shedding kinetics were similar, with higher viral loads from Op swabs than C swabs. H5N1-W2 showed a more prolonged Op shedding period, though total viral load did not differ significantly between groups. Notably, H5N8-W2 caused 50% mortality, while H5N1-W2 caused none. Previous studies have shown that an earlier H5N1-W2 HPAIV (genotype C) had comparable infectivity and transmissibility to other clade 2.3.4.4 HPAIVs, with enhanced fitness in Anseriformes [30–32]. Recently, Bordes *et al.* [33] compared two H5N1 genotypes of different dominance [genotype C (wave 1 – low) and genotype AB (wave 2 – high)] in three species of Anseriformes [Pekin ducks (*A. platyrhynchos*), Eurasian wigeon (*Mareca penelope*) and barnacle geese (*Branta leucopsis*)] [33]. In all three species, the dominant genotype AB was less pathogenic than the less dominant genotype C; in Pekin ducks, no mortalities were seen for genotype AB compared with 40% mortalities with genotype C. The observation of high mortalities with early wave 1 H5N1 (genotype C) parallels our findings of high mortalities for early wave 1 H5N8. Furthermore, consistent with our observations here, viral shedding kinetics were comparable between genotype AB and genotype C [33]. Bordes *et al.* [33] did not assess transmission dynamics, and likewise, transmission was not assessed here in our study. However, several studies highlighted a correlation between transmission efficiency and the extent of environmental contamination, particularly in water sources, for H5Nx 2.3.4.4b viruses [23, 31]. In our study, environmental contamination, particularly of the pond and drinking water, was detected more frequently with H5N1-W2. This, combined with reduced vRNA shedding duration and higher mortality for H5N8-W2, suggests that H5N1-W2 may transmit more efficiently in wild waterfowl. The infrequent contact between wild birds implies that premature host death could limit transmission opportunities, as previously proposed [34]. It has been suggested that HPAIV infection within a breeding colony may alter host behaviour and change spacing between colonies; thus, changes in use of breeding grounds may potentially have favoured transmission of H5N1-W2 over H5N8-W2 [35, 36]. Together, these data indicate phenotypic differences between H5N8 and H5N1 that may explain the ecological shift in subtype dominance from H5N8 in wave 1 to H5N1 in wave 2 in the UK and Europe.

Following initial characterization of infection dynamics and pathogenicity, we investigated the potential role of antibody-mediated immunity in the observed shift in subtype prevalence between the first two outbreak waves. Some avian species are susceptible to HPAIV yet can survive infection. Ringing data suggest wild Anseriformes have life expectancies ranging from 3 to 20 years, depending on species [37], implying that individuals tolerant to infection may persist across multiple epizootics and encounter diverse AIV subtypes and genotypes [23, 38]. Antigenic relatedness and associated cross-reactivity between similar HA and/or NA proteins can complicate the interpretation of serological data in wild birds. Nevertheless, HA- and NA-specific antibodies have been detected in several wild waterfowl species [31, 39, 40]. To explore this further, we first assessed serological responses

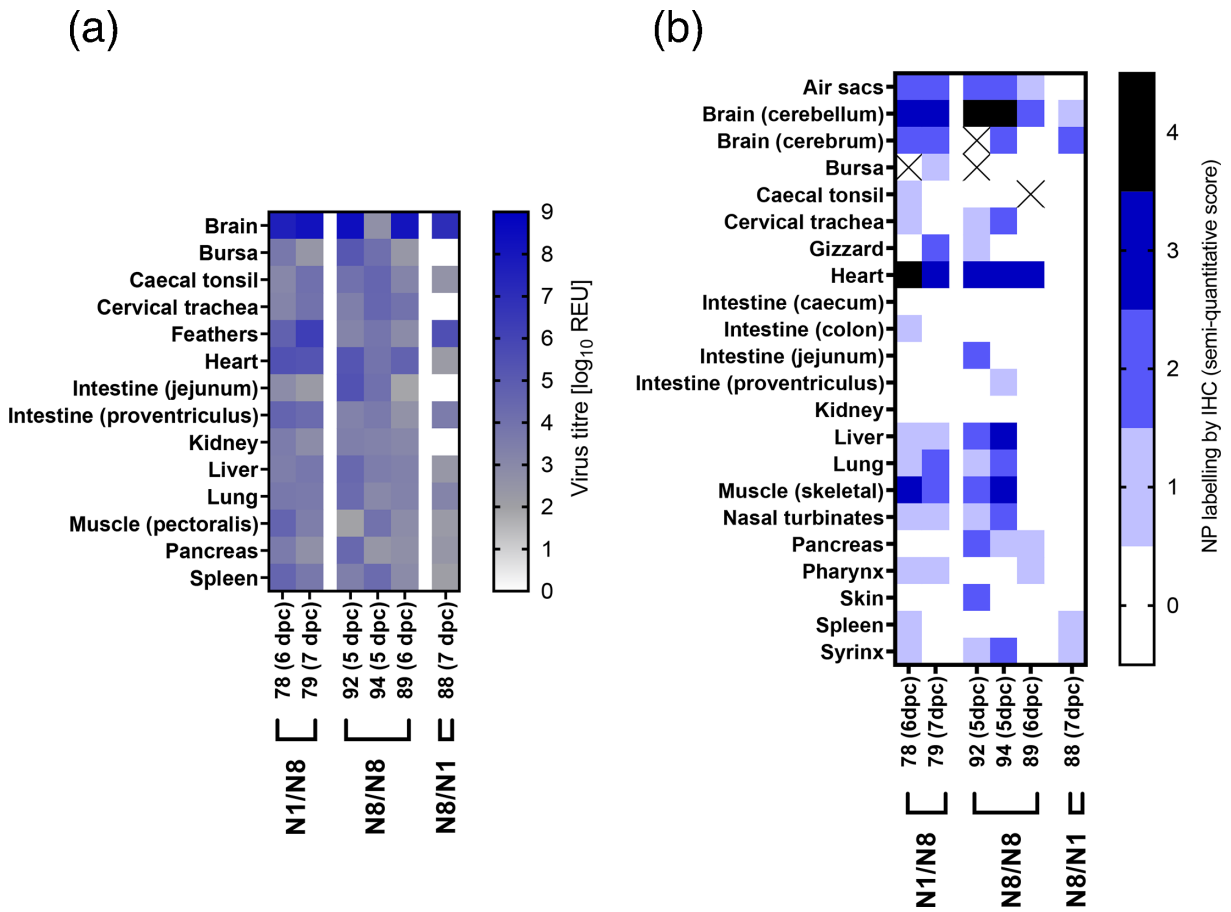

Fig. 7. Organ tropism in ducks with prior exposure to de-engineered AIVs before H5N1-W2 and H5N8-W2 HPAIV challenge. Tissue samples were collected from six ducks following H5N1-W2 or H5N8-W2 HPAIV challenge, which had previously been exposed to a homologous (N1/N1 and N8/N8) or heterologous (N1/N8 and N8/N1) subtype of de-engineered H5N1-W1 or H5N8-W1 AIVs. All ducks were euthanized at indicated times (dpc) as a result of severe clinical signs. (a) vRNA levels, measured by M-gene RT-PCR, expressed as $\log_{10}$ REU and represented as a heatmap. Samples below the diagnostic cut-off ($10^{1.794}$ REU) are shown in grey, positive samples in blue and no Ct in white. Individual bird identifiers allow for comparisons to serological response graphs and IHC staining results. (b) Semi-quantitative scoring of anti-NP staining intensities and distribution in IHC analysis of tissues (lower to higher intensities, 0-4), demonstrating abundant viral antigen in the brain, heart and muscle following N1/N8 and N8/N8 challenge.

in naïve ducks surviving infection with H5N1-W2 or H5N8-W2, finding that all birds seroconverted by HI. Although not statistically significant, titres were lower when sera from both groups were evaluated against H5N8-W2 antigen than H5N1-W2. To better resolve HA-specific responses, we evaluated antibody titres using HA-only PVNAs. No significant differences in IC_{50} values were observed between sera from H5N1 and H5N8-infected birds. This similarity in HA antigenicity among clade 2.3.4.4b H5Nx viruses aligns with previous findings [41, 42] and likely reflects the high AA identity across their HA proteins (Table S3).

Although most of the antibody response in birds exposed to AIV targets HA [43], antibodies against NA also contribute to protective immunity [44, 45]. However, the composition and function of the antibody repertoire in wild bird species remain poorly characterized, particularly regarding the relative roles of HA- and NA-specific responses in protection. To investigate this, we assessed NA-specific antibodies using the pELLA assay [29]. While pELLA does not directly quantify neutralization, it correlates well with NA inhibition activity [29, 44, 45]. Sera from ducks surviving infection showed detectable NA-specific antibodies, indicating a reactive immune response to NA [46, 47]. Previous studies have demonstrated a protective role for NA antibodies in Canada geese (*Branta canadensis*) and mallards (*A. platyrhynchos*), where prior low pathogenicity AIV (LPAIV) exposure reduced disease severity upon NA-homologous H5Nx HPAIV challenge [46, 47]. Similarly, NA antibodies have provided protection against H5N1 HPAIV in chickens [48]. These findings support the concept of 'permissive immunity', whereby NA antibodies limit viral release from infected cells, thereby mitigating disease without fully blocking infection [49, 50], in line with our observations. Additionally, neutralizing NA antibodies against N1 and N8 have been detected in wild ducks in North America [51]. Interestingly, H5N1-W2-specific antisera in our study exhibited broader cross-subtype reactivity, inhibiting both H5N1 and H5N8 PVs, while H5N8-W2 antisera reacted only with homologous PVs. Importantly, while the PVs used in this

study possessed the same HA subtype (both containing an H5 HA with different NA subtypes), HA interference in the pELLA has not previously been reported [29]. Therefore, together, this raises the hypothesis that NA-reactive antibodies may persist following H5Nx infection, with H5N1-induced antibodies conferring broader cross-reactivity. Notably, this pattern mirrors the epidemiological shift from H5N8 to H5N1 dominance between waves 1 and 2, raising the possibility that immunity to H5N8 may have facilitated the emergence of H5N1 by allowing subsequent infection in previously exposed hosts.

To further examine the impact of prior subtype exposure on infection outcome, we de-engineered the MBCS of H5N1-W1 and H5N8-W1 HPAIVs to contain an SBCS, minimizing potential severe outcomes in ducks. The low pathogenicity phenotype of both mutants was confirmed by IVPI, as per international guidelines [52]. Unexpectedly, for ducks inoculated with 10^7 EID_{50} of these de-engineered viruses, no viral shedding or seroconversion was detected. This contrasted with chickens in the IVPI, which developed robust serological responses, including one mortality with vRNA detected in multiple tissues, while retaining the SBCS in HA. Additionally, *in ovo* amplification produced similar viral titres for both WT and de-engineered viruses, together suggesting the modified viruses remained replication competent in animal systems. Collectively, while different administration routes were used for the chickens and ducks, these findings suggest that while the viruses are viable, the MBCS is essential for productive infection of ducks via intranasal administration with clade 2.3.4.4b H5Nx viruses.

The lack of seroconversion to the de-engineered viruses was unexpected. However, other host responses outside of antibody generation are also likely important for infection outcome following AIV infection [53], and so we investigated the effect of homosubtypic and heterosubtypic re-infection. However, prior exposure had a limited impact on vRNA shedding following HPAIV challenge. However, in the N1/N1 group, shedding and environmental contamination were delayed compared with naïve H5N1-W2-infected ducks, with fewer positive C swabs. This delay was more pronounced in homologous (N1/N1) than heterologous (N1/N8) challenge (4 vs. 2 days, respectively). Disease severity also varied depending on the priming subtype. Prior SB-H5N1-W1 exposure reduced clinical scores and mortality following challenge with either H5N1-W2 or H5N8-W2. Conversely, prior SB-H5N8-W1 exposure increased disease severity and mortality for both challenge viruses. This may reflect differences in (i) infection efficiency of the challenge virus, (ii) replication of the SB-H5N8-W1 virus or (iii) host immune modulation and the clonal nature of the priming vs. challenge viruses. Earlier studies found that pre-exposure to LPAIV, especially with seroconversion, conferred protection from HPAIV-induced disease [11, 54, 55], though these studies used older birds (13 weeks–18 months) compared with the 3-week-old ducks used here. Age-related immune differences, particularly within the first 6 weeks post-hatch [56–58], therefore may explain the differences observed. In the N8/N8 group, we obtained inverse results following challenge, with the pre-exposed birds having higher mortality than the naïve/N8 group. Unlike previous exposure studies that used genetically distinct LPAIVs [11, 55, 59], in the current study, we used RG to de-engineer the MBCS and retain close genetic relationships between de-engineered AIV W1 exposure and HPAIV W2 challenge.

Interestingly, we observed differences in clinical outcomes following challenge with WT HPAIVs, despite the absence of detectable antibodies against the de-engineered virus used in the prior-exposure inoculation. Similarly, a recent study observed that ducks previously experimentally exposed to either H5N1 or H5N8 were protected against heterologous challenge with H5N1 or H5N8 HPAIVs, despite lacking detectable antibodies against the challenge virus following initial exposure [60]. Moreover, in another study, mallards exposed to H4N6 reported minimal detectable antibody responses but identified early activation of the complement system during infection [61]. Collectively, these findings align with our data and suggest the involvement of alternative immunological mechanisms in ducks that may modulate disease outcomes following prior exposure to H5Nx HPAIV. It is plausible that such prior infections influence innate or cellular immunity, rather than eliciting strong humoral responses. Unfortunately, due to limited sample availability and the lack of appropriate reagents for immunological characterization in ducks, we were unable to investigate these mechanisms in greater detail. Further, methods used to inactivate sera to enable removal of samples from high containment facilities likely render the material unsuitable for testing cytokine levels, and as such, retrospective assessment could not be undertaken. Nonetheless, the role of innate and cellular immunity in shaping the outcome of HPAIV infections in ducks clearly warrants further investigation and should be a key focus in future studies of this nature. While the exact mechanism remains uncertain, prior exposure does not greatly impact viral shedding but does appear to alter disease severity. While cross-subtype immunization and challenge has been reported to cause vaccine-associated enhanced respiratory disease (VAERD) in pigs and ferrets [62, 63], there have been no reports of VAERD in avian hosts, but subtype mismatch during our prior exposure and challenge has shown an increase in clinical scores. When considering the epidemiological switch in dominance from H5N8 to H5N1, birds would potentially be exposed to H5N8 and subsequently encounter H5N1. In this scenario, our data suggest that prior exposure to H5N8 may not protect against subsequent exposure to H5N8 but could allow ducks to tolerate H5N1 infection, although allowing infection and transmission of H5N1 among Anseriformes. All N8/N1 ducks shed H5N1-W2 to similar titres as the H5N1-W2 naïve birds, but 80% survived infection.

In conclusion, this study identifies distinct virological and serological differences between H5N1-W2 and H5N8-W2 that may explain the rapid shift in subtype dominance during the 2021–2022 epizootic in the UK and continental Europe. While both viruses demonstrated comparable shedding kinetics and environmental contamination in infected ducks as surrogates for wild Anseriformes, H5N8-W2 exhibited higher pathogenicity, leading to greater mortality. However, the delayed onset of shedding and the increased survival associated with H5N1-W2 suggest that H5N1 may be more adept at sustaining transmission, particularly

in wild bird populations. Furthermore, NA-reactive antibodies were detected following infection with both subtypes. Notably, N1 antisera cross-reacted with N8, but the reverse was not observed, suggesting that prior H5N8 exposure may not impede subsequent H5N1 infection at the wild waterfowl population scale. In addition, prior exposure may enhance the severity of disease outcome outside of humoral responses, though mechanisms are unknown. Together, these data suggest that in ducks, genotype A H5N8 from the second epizootic wave is more pathogenic than genotype AB H5N1 from the same period and that H5N1 pathogenicity has decreased between epizootic waves, whereas H5N8 pathogenicity has been maintained or increased. These phenotypic characteristics could favour selection of H5N1 in a partially immune H5N8 population, but the ability of H5N1 viruses to at least in part evade host antibody responses to H5N8 could create an environment in the natural reservoir favouring their selection and persistence. These factors may have a direct correlation with the emergence and complete shift to H5N1 HPAIVs where previously H5N8 was dominant.

Following initial selection and shift, H5N1 rapidly underwent reassortment to produce a highly variable number of genotypes that also has likely contributed to the rapid dissemination and spread of this subtype [10]. H5N1 has continued to emerge, reassort and genetically evolve with LPAIVs present in wild birds, co-existing as multiple genotypes that, through increasing opportunity for infection and fitness in multiple avian species, remain in dynamic circulation on a global scale. These insights underscore the complex interplay of viral fitness, host immunity and environmental factors in shaping the dynamics of gsGD lineage H5Nx HPAIV epizootics. Certainly, a more robust assessment of different HPAIV genotypes is required to understand the impact of these viruses on different avian populations.

Funding information
This work was supported by the Biotechnology and Biological Sciences Research Council (BBSRC) and Department for Environment, Food and Rural Affairs (Defra, UK) research initiative 'FluMAP' and 'FluTrailMap' (grant nos. BB/X006204/1 and BB/Y007271/1, respectively). Funding was also provided by the Defra and the Devolved Administrations of Scotland and Wales, through SE2213 'FLUFUTURES 2' and SE2227 'FluFocus'. The work was also supported by the BBSRC grants BBS/E/PI/230001B, BBS/E/PI/230002C, BBS/E/PI/23NB0004 and BBS/E/PI/23NB0003.

Acknowledgements
The authors would like to thank Nadia Chew, Amy Miller and Elena Mather for the collection and processing of samples from the *in vivo* experiments and the post-mortem and histopathology teams in the Pathology Department for the collection and processing of tissues.

Author contributions
E.B., C.J.W., S.S.T., S.J., S.R., A.-L.S., A.N., J.J. and M.J.S. conducted the in vivo experimental work. C.D.G., E.B. and S.S.T. conducted serological work. J.Y. and M.I. produced the viruses by reverse genetics. N.T. and K.d.C. provided logistical support and training for PVNA and pELLA. E.B., C.J.W., A.M.P.B., J.J., M.J.S. and C.D.G. analysed the data. E.B., C.J.W., C.D.G., M.J.S., I.H.B., A.C.B. and J.J. wrote the manuscript. J.J., A.C.B. and I.H.B. secured funding. D.D.S. and J.P. conducted *in vivo* work; M.A. conducted serological work

Conflicts of interest
The authors declare no conflicts of interest.

Ethical statement
The *in vivo* study was reviewed and approved by the local Animal and Plant Health Agency (APHA) Animal Welfare and Ethical Review Body (AWERB) to comply with the relevant UK legislation, in accordance with the UK Home Office (HO) Project License PP7633638. Material utilized for all experimentation was initially isolated in EFEs under HO license P5275AD31. According to the UK's Advisory Committee on Dangerous Pathogens (ACDP) and the Specified Animal Pathogens Order (SAPO), the gsGd lineage H5Nx HPAIVs are classified as ACDP hazard group level 3 pathogens and SAPO level 4; hence, all animal and laboratory work involving infectious material was conducted within licensed containment level 3 facilities at APHA. Welfare monitoring of up to three times daily was undertaken to assess the birds for humane endpoints following the onset of clinical disease, enabling any decisions to be made concerning the need for euthanasia. All birds had access to food and water *ad libitum*.

References

1. Fereidouni S, Starick E, Karamendin K, Genova CD, Scott SD, *et al*. Genetic characterization of a new candidate hemagglutinin subtype of influenza A viruses. *Emerg Microbes Infect* 2023;12:2225645.
2. Shi W, Lei F, Zhu C, Sievers F, Higgins DG. A complete analysis of HA and NA genes of influenza A viruses. *PLoS one* 2010;5:e14454.
3. Xie R, Edwards KM, Wille M, Wei X, Wong S-S, *et al*. The episodic resurgence of highly pathogenic avian influenza H5 virus. *Nature* 2023;622:810–817.
4. Adlhoch C, Gossner C, Koch G, Brown I, Bouwstra R, *et al*. Comparing introduction to Europe of highly pathogenic avian influenza viruses A(H5N8) in 2014 and A(H5N1) in 2005. *Euro Surveill* 2014;19:20996.
5. Adlhoch C, Fusaro A, Gonzales JL, Kuiken T, Marangon S, *et al*. Avian influenza overview March - June 2022. *EFSA J* 2022;20:e07415.
6. Adlhoch C, Brouwer A, Kuiken T, Mulatti P, Smietanka K, *et al*. Avian influenza overview February - May 2018. *EFSA J* 2018;16:e05358.
7. Beerens N, Koch G, Heutink R, Harders F, Vries DPE, *et al*. Novel highly pathogenic avian influenza A(H5N6) virus in the Netherlands, December 2017. *Emerg Infect Dis* 2018;24:770–773.
8. Śmietanka K, Świętoń E, Kozak E, Wyrostek K, Tarasiuk K, *et al*. Highly pathogenic avian influenza H5N8 in Poland in 2019-2020. *J Vet Res* 2020;64:469–476.
9. Adlhoch C, Fusaro A, Gonzales JL, Kuiken T, Marangon S, *et al*. Avian influenza overview February - May 2021. *EFSA J* 2021;19:e06951.
10. Byrne AMP, James J, Mollett BC, Meyer SM, Lewis T, *et al*. Investigating the genetic diversity of H5 avian influenza viruses in the United Kingdom from 2020–2022. *Microbiol Spectr* 2023;11:e04776–04722.
11. Caliendo V, Leijten L, van de Bildt MWG, Poen MJ, Kok A, *et al*. Long-term protective effect of serial infections with H5N8 highly pathogenic avian influenza virus in wild ducks. *J Virol* 2022;96:e0123322.
12. European Reference Laboratory (EURL). EURL: avian flu data portal; 2025. https://eurlaidata.izsvenezie.it/epidemio.php#:~:text=wild%20birds%20cases.-,Genotypes,genotypes%20present%20in%20each%20country [accessed 6 January 2025].

13. Adlhoch C, Fusaro A, Gonzales JL, Kuiken T, Marangon S, *et al*. Avian influenza overview December 2021 - March 2022. *EFSA J* 2022;20:e07289.
14. The Animal And Plant Health Agency (APHA). Updated outbreak assessment #44 high pathogenicity avian influenza (HPAI) in the UK and Europe; 2023. https://assets.publishing.service.gov.uk/media/64b6905671749c000d89ed78/11_July_2023_High_pathogenicity_avian_influenza_HPAI_in_Europe.pdf [accessed 5 March 2025].
15. Arter-Hazzard M, Burns G, Adridge C, Gale DP, Perrin DL, *et al*. Updated outbreak assessment #46 high pathogenicity avian influenza (HPAI) in the UK and europe; 2023
16. The Animal And Plant Health Agency (APHA). Updated outbreak assessment #34 high pathogenicity avian influenza (HPAI) in the UK and Europe; 2022. https://assets.publishing.service.gov.uk/media/634d89e2e90e0731a8008917/HPAI_Europe__34_10_October_2022_FINAL__003_.pdf [accessed 5 March 2025].
17. The Animal And Plant Health Agency (APHA). Updated outbreak assessment #27 high pathogenicity avian influenza (HPAI) in the UK and Europe; 2022. https://assets.publishing.service.gov.uk/media/62a35fe0d3bf7f037097bece/HPAI_Europe_6_June_2022.pdf [accessed 5 March 2025].
18. The Animal And Plant Health Agency (APHA). Updated outbreak assessment #38 high pathogenicity avian influenza (HPAI) in the UK and Europe; 2023. https://assets.publishing.service.gov.uk/media/63bd54458fa8f55e362ce02f/hpai-europe-number38-230104.pdf [accessed 5 March 2025].
19. Pohlmann A, King J, Fusaro A, Zecchin B, Banyard AC, *et al*. Has epizootic become enzootic? Evidence for a fundamental change in the infection dynamics of highly pathogenic avian influenza in Europe, 2021. *mBio* 2022;13:e0060922.
20. James J, Bhat S, Walsh SK, Karunarathna TK, Sadeyen J-R, *et al*. The origin of internal genes contributes to the replication and transmission fitness of H7N9 avian influenza virus. *J Virol* 2022;96:e0129022.
21. World Organisation for Animal Health (WOAH). Terrestrial manual: chapter 3.3.4. Avian influenza (including infection with high pathogenicity avian influenza viruses); 2021. https://www.woah.org/fileadmin/Home/eng/Health_standards/tahm/3.03.04_AI.pdf
22. Nagy A, Černíková L, Kunteová K, Dirbáková Z, Thomas SS, *et al*. A universal RT-qPCR assay for "One Health" detection of influenza A viruses. *PLoS One* 2021;16:e0244669.
23. James J, Billington E, Warren CJ, De Sliva D, Di Genova C, *et al*. Clade 2.3.4.4b H5N1 high pathogenicity avian influenza virus (HPAIV) from the 2021/22 epizootic is highly duck adapted and poorly adapted to chickens. *J Gen Virol* 2023;104.
24. Löndt BZ, Nunez A, Banks J, Nili H, Johnson LK, *et al*. Pathogenesis of highly pathogenic avian influenza A/turkey/Turkey/1/2005 H5N1 in Pekin ducks (Anas platyrhynchos) infected experimentally. *Avian Pathol* 2008;37:619–627.
25. James J, Warren CJ, De Silva D, Lewis T, Grace K, *et al*. The role of airborne particles in the epidemiology of clade 2.3.4.4b H5N1 high pathogenicity avian influenza virus in commercial poultry production units. *Viruses* 2023;15:1002.
26. James J, Slomka MJ, Reid SM, Thomas SS, Mahmood S, *et al*. Development and application of real-time PCR assays for specific detection of contemporary avian influenza virus subtypes N5, N6, N7, N8, and N9. *Avian Dis* 2018;63:209.
27. Del Rosario JMM, da Costa KAS, Asbach B, Ferrara F, Ferrari M, *et al*. Exploiting pan influenza A and pan influenza B pseudotype libraries for efficient vaccine antigen selection. *Vaccines* 2021;9:741.
28. James J, Rhodes S, Ross CS, Skinner P, Smith SP, *et al*. Comparison of serological assays for the detection of SARS-CoV-2 antibodies. *Viruses* 2021;13:713.
29. da Costa KAS, Del Rosario JMM, Ferrari M, Vishwanath S, Asbach B, *et al*. Influenza A (N1-N9) and influenza B (B/Victoria and B/Yamagata) neuraminidase pseudotypes as tools for pandemic preparedness and improved influenza vaccine design. *Vaccines* 2022;10:1520.
30. Puranik A, Slomka MJ, Warren CJ, Thomas SS, Mahmood S, *et al*. Transmission dynamics between infected waterfowl and terrestrial poultry: differences between the transmission and tropism of H5N8 highly pathogenic avian influenza virus (clade 2.3.4.4a) among ducks, chickens and turkeys. *Virology* 2020;541:113–123.
31. Seekings AH, Warren CJ, Thomas SS, Mahmood S, James J, *et al*. Highly pathogenic avian influenza virus H5N6 (clade 2.3.4.4b) has a preferable host tropism for waterfowl reflected in its inefficient transmission to terrestrial poultry. *Virology* 2021;559:74–85.
32. Slomka MJ, Puranik A, Mahmood S, Thomas SS, Seekings AH, *et al*. Ducks are susceptible to infection with a range of doses of H5N8 highly pathogenic avian influenza virus. *Avian Dis* 2016;63:172–180.
33. Bordes L, Germeraad EA, Roose M, van Eijk NMHA, Engelsma M, *et al*. Experimental infection of chickens, Pekin ducks, Eurasian wigeons and Barnacle geese with two recent highly pathogenic avian influenza H5N1 clade 2.3.4.4b viruses. *Emerg Microbes Infect* 2024;13:2399970.
34. James J, Howard W, Iqbal M, Nair VK, Barclay WS, *et al*. Influenza A virus PB1-F2 protein prolongs viral shedding in chickens lengthening the transmission window. *J Gen Virol* 2016;97:2516–2527.
35. Falchieri M, Reid SM, Ross CS, James J, Byrne AMP, *et al*. Shift in HPAI infection dynamics causes significant losses in seabird populations across Great Britain. *Vet Rec* 2022;191:294–296.
36. Jeglinski JWE, Lane JV, Votier SC, Furness RW, Hamer KC, *et al*. HPAIV outbreak triggers short-term colony connectivity in a seabird metapopulation. *Sci Rep* 2024;14:3126.
37. BirdFacts: key information about the UK's birds and their changing fortunes, based on data collected by BTO and partner organisations; 2024. https://www.bto.org/understanding-birds/birdfacts/mallard [accessed 6 February 2024].
38. Wade D, Ashton-Butt A, Scott G, Reid SM, Coward V, *et al*. High pathogenicity avian influenza: targeted active surveillance of wild birds to enable early detection of emerging disease threats. *Epidemiol Infect* 2022;151:e15.
39. Magor KE. Immunoglobulin genetics and antibody responses to influenza in ducks. *Dev Comp Immunol* 2011;35:1008–1017.
40. Greco F, Ravenswater HM, Ruiz-Raya F, D'Avino C, Newell MA, *et al*. Asymptomatic infection and antibody prevalence to co-occurring avian influenza viruses vary substantially between sympatric seabird species following H5N1 outbreaks. *Ecology* 2024. DOI: 10.1101/2024.09.26.614314.
41. Yang J, Daines R, Chang P, Karunarathna TK, Qureshi M, *et al*. The haemagglutinin genes of the UK clade 2.3.4.4b H5N1 avian influenza viruses from 2020 to 2022 retain strong avian phenotype. *bioRxiv*;2024:2024.
42. OFFLU (Joint OIE (World Organisation for Animal Health) and FAO (Food and Agriculture Organization of the United Nations) network of expertise on animal influenza. OFFLU avian influenza Matching (AIM) Technical Report, July 2024; 2024. https://offlu.org/technical-activities/offlu-aim-technical-report-july-2024/ [accessed 24 March 2025].
43. Philpott M, Easterday BC, Hinshaw VS. Neutralizing epitopes of the H5 hemagglutinin from a virulent avian influenza virus and their relationship to pathogenicity. *J Virol* 1989;63:3453–3458.
44. Rott R, Becht H, Orlich M. The significance of influenza virus neuraminidase in immunity. *J Gen Virol* 1974;22:35–41.
45. McNulty MS, Allan GM, Adair BM. Efficacy of avian influenza Neuraminidase-specific vaccines in chickens. *Avian Pathol* 1986;15:107–115.
46. Berhane Y, Embury-Hyatt C, Leith M, Kehler H, Suderman M, *et al*. Pre-exposing Canada Geese (*Branta canadensis*) to a low-pathogenic H1N1 avian influenza virus protects them against H5N1 HPAI virus challenge. *J Wildl Dis* 2014;50:84–97.
47. Tarasiuk K, Kycko A, Świętoń E, Bocian Ł, Wyrostek K, *et al*. Homo- and heterosubtypic immunity to low pathogenic avian influenza virus mitigates the clinical outcome of infection with

highly pathogenic avian influenza H5N8 clade 2.3.4.4.b in Captive Mallards (*Anas platyrhynchos*). *Pathogens* 2023;12:217.

48. Luczo JM, Spackman E. Epitopes in the HA and NA of H5 and H7 avian influenza viruses that are important for antigenic drift. *FEMS Microbiol Rev* 2024;48:fuae014.
49. Johansson BE, Kilbourne ED. Dissociation of influenza virus hemagglutinin and neuraminidase eliminates their intravirionic antigenic competition. *J Virol* 1993;67:5721–5723.
50. Johansson BE, Bucher DJ, Kilbourne ED. Purified influenza virus hemagglutinin and neuraminidase are equivalent in stimulation of antibody response but induce contrasting types of immunity to infection. *J Virol* 1989;63:1239–1246.
51. Stallknecht DE, Fojtik A, Carter DL, Crum-Bradley JA, Perez DR, *et al*. Naturally acquired antibodies to influenza A virus in fall-migrating North American Mallards. *Vet Sci* 2022;9:214.
52. World Organisation for Animal Health (WOAH). Terrestrial manual: avian influenza (infection with avian influenza viruses); 2019 [accessed 26 November 2019].
53. Dai M, Sun H, Zhao L, Wu Q, You B, *et al*. Duck $CD8^+$ T cell response to H5N1 highly pathogenic avian influenza virus infection in vivo and in vitro. *J Immunol* 2022;209:979–990.
54. Fereidouni SR, Starick E, Beer M, Wilking H, Kalthoff D, *et al*. Highly pathogenic avian influenza virus infection of mallards with homo- and heterosubtypic immunity induced by low pathogenic avian influenza viruses. *PLoS One* 2009;4:e6706.
55. Koethe S, Ulrich L, Ulrich R, Amler S, Graaf A, *et al*. Modulation of lethal HPAIV H5N8 clade 2.3.4.4B infection in AIV pre-exposed mallards. *Emerg Microbes Infect* 2020;9:180–193.
56. Zhang A, Xu J, Lai H, Huang W, Fang N, *et al*. Age-related changes and distribution of T cell markers (CD3 and CD4) and toll-like receptors(TLR2, TLR3,TLR4 and TLR7) in the duck lymphoid organs. *Immunobiology* 2017;222:857–864.
57. Liang S, Lu M, Yu D, Xing G, Ji Z, *et al*. Effects of age on differential resistance to duck hepatitis A virus genotype 3 in Pekin ducks by 16 S and transcriptomics. *Comput Struct Biotechnol J* 2024;23:771–782.
58. Lv C, Li R, Liu X, Li N, Liu S. Pathogenicity comparison of duck Tembusu virus in different aged Cherry Valley breeding ducks. *BMC Vet Res* 2019;15:282.
59. Hansen R, Brown I, Brookes S, Welchman D, Cromie R. Current status of avian influenza in Europe and the UK. *Vet Rec* 2018;182:54–55.
60. Sakuma S, Mine J, Uchida Y, Kumagai A, Takadate Y, *et al*. Long-term immune responses induced by low-dose infection with high pathogenicity avian influenza viruses can protect mallards from reinfection with a heterologous strain. *Arch Virol* 2025;170:33.
61. van Dijk JGB, Verhagen JH, Hegemann A, Tolf C, Olofsson J, *et al*. A comparative study of the innate humoral immune response to avian influenza virus in wild and domestic mallards. *Front Microbiol* 2020;11:608274.
62. Khurana S, Loving CL, Manischewitz J, King LR, Gauger PC, *et al*. Vaccine-induced anti-HA2 antibodies promote virus fusion and enhance influenza virus respiratory disease. *Sci Transl Med* 2013;5.
63. Kimble JB, Wymore Brand M, Kaplan BS, Gauger P, Coyle EM, *et al*. Vaccine-associated enhanced respiratory disease following influenza virus infection in ferrets recapitulates the model in pigs. *J Virol* 2022;96.